J Mater Sci (2011) 46:1095–1102
DOI 10.1007/s10853-010-4878-5

Structural and dielectric properties of Li_2O–ZnO–BaO–B_2O_3–CuO glasses

Shaaban M. Salem · E. M. Antar · E. A. Mohamed

Received: 22 March 2010 / Accepted: 28 August 2010 / Published online: 22 September 2010

Abstract Glass samples of the system ($15Li_2O$–30ZnO–10BaO–$(45 - x)B_2O_3$–xCuO where $x = 0$, 5, 10 and 15 mol%) were prepared by using the melt quenching technique. A number of studies, viz. density, differential thermal analysis, FT-IR spectra, a.c. conductivity and dielectric properties (constant $\varepsilon\varphi$, loss tan δ, a.c. conductivity, σ_{ac}, over a wide range of frequency and temperature) of these glasses were carried out as a function of copper ion concentration. The analysis of the results indicate that the density increases while molar volume decreases with increasing of copper content indicates structural changes of the glass matrix. The glass transition temperature, T_g, and crystallization temperature, T_c, increase with the variation of concentration of CuO referred to the growth in the network connectivity in this concentration range, while glass-forming ability parameter ($T_c - T_g$) decreases with increasing CuO content, indicates an increasing concentration of copper ions that take part in the network-modifying positions. The FT-IR spectra evidenced that the main structural units are BO_3, BO_4, and ZnO_4. The structural changes observed by varying the CuO content in these glasses and evidenced by FTIR investigation suggest that the CuO plays a network modifier role in these glasses while ZnO plays the role of network formers. The dielectric constant decreased with increase in temperature and CuO content. The variation of a.c. conductivity with the concentration of CuO passes through a maximum at 5 mol%. In the high temperature region, the a.c. conduction seems to be connected with the mixed conduction viz., electronic conduction and ionic conduction.

S. M. Salem (✉)
Department of Physics, Faculty of Science, Al Azhar University, Nasr City, Cairo 11884, Egypt
e-mail: shaabansalem@gmail.com

E. M. Antar
Radiation Protection and Dosimetry Department, National Center for Radiation Research & Technology, AEA, Nasr City, Cairo, Egypt

E. A. Mohamed
Department of Physics, Faculty of Science (Girl's Branch), Al Azhar University, Nasr City, Cairo, Egypt

Introduction

Borate glasses containing Li^+ have been extensively studied due to their technological applications as solid electrolyte in electro chemical devices such as batteries [1]. Alkali borate glasses are highly useful materials for vacuum ultra violet optics and semiconductors lithography owing to the presence of stable glass forming range and transparency from the near UV to the middle infrared region [2]. Alkali/alkaline earth borate glasses containing various transition metal ions have been under extensive investigation of their technological applications especially in phosphors, lasers, solar energy converters, and in a number of electronic devices. The reason is that, in the glasses the transition metal ion can exist in more than one valence state [3–6]. These glasses are relatively resistant to atmospheric moisture and are capable of accepting large concentrations of transition metal ions, rare earth ions, and can be composed of structural groupings (boroxol, tetraborate, diborate, metaborate, pyroborate, and orthoborate) that are present in the various crystal structures of the alkali borate compounds. The addition of alkali oxides modifies the boroxol rings, which are complex borate groups with one or two four coordinated boron atoms [7]. Transition metal ions are very interesting ions to probe in the glass network because their

outer *d*-electron orbital functions have rather broad radial distributions and their responses to surrounding stimuli are very sensitive to the ions positions. As a result, these ions influence the physical properties of the glasses to a substantial extent. Copper is being extensively used in several commercial glasses, such as red glass hematite, aventurine, and rubies. CuO containing glasses are also important in technological point of view, because of semiconducting properties and due to other potential applications [8, 9].

In glasses, copper ions exist in two stable ionic states viz., monovalent Cu^{+} ions and divalent Cu^{2+} ions and may also exist as metallic copper. The electronic structure of the copper atom is [Ar] $3d^{10}\,4s^{1}$; the cuprous ion, having its five *d*-orbitals occupied, does not produce coloring [10], while Cu^{2+} ions create color centers with an absorption band in the visible region [11, 12] and produce blue and green glasses. The color of the glass depends on the Cu^{2+} content, its specific coordination, composition, and basicity of the glass. Colors produced by Cu^{2+} ions in various glasses have been interpreted [13] in terms of ligand field theory. Though, a reasonably good number of recent studies on the environment of copper ions in a variety of inorganic glass systems are available [14–17] including zinc borate glasses [18], most of them are focused on structural investigations by means of Raman and IR spectroscopic studies. Virtually, no studies are available on dielectric properties of zinc borate glasses containing copper ions. The study of dielectric properties such as dielectric constant, ε', loss, tan δ, and a.c. conductivity, σ_{ac}, over a wide range of frequency and temperature of the glass materials not only helps in assessing the insulating character and understanding the conduction phenomenon but also throws light on the structural aspects of the glasses to a large extent. The objective of this paper is to have a comprehensive understanding over the topology and valence states of copper ions and to throw some light on a.c. conduction phenomenon in $(15Li_2O–30ZnO–10BaO–(45 - x)B_2O_3–xCuO$ where $x =$ 0, 5, 10, and 15 mol%) glass system, by a systematic study of physical and dielectric properties coupled with spectroscopic investigations of IR spectra.

Experimental

The glass samples of the formula $(15Li_2O–30ZnO–10BaO–(45 - x)B_2O_3–xCuO$ where $x = 0$, 5, 10, and 15mol%) have been prepared by the melt quenching technique. Required quantities of analytical grade Li_2CO_3, ZnO H_3BO_3, and CuO were mixed together by grinding the mixture repeatedly to obtain a fine powder. The mixture is melted in porcelain crucible at about 1473 K for about 30 min to homogenize the melt. The melt was quickly quenched by pouring on to a stainless steel plate and covering with another stainless steel plate and the random pieces of samples thus formed were collected. Density, *d*, at room temperature was measured by following Archimedes principle using a sensitive single pan balance (Sartorius). The carbon tetrachloride, CCl_4 (density = 1.595 m/cc) was used as an immersion liquid. The molar volume (V_m) and concentration of copper ions, N (cm^{-3}), were calculated as $N = [dPN_A/100A_w]$, where N_A is Avogadro's number, p the weight percentage of atoms, A_w is the atomic weight, and d is the density. The thermal behavior was investigated using a Shimadzu DTA-50 differential thermal analysis. The temperature and energy calibrations of the instrument were performed using the well known melting temperatures and melting enthalpies of high purity tin, lead, and indium supplied with the instrument. Samples in the form of powders weighing around 20 mg were sealed in platinum pans in an atmosphere of dry nitrogen at a flow of 30 mL/min and scanned from room temperature to above the exothermic peak at heating rate of 10 °C/min. The values of the glass transition temperature, T_g, and the peak temperature of crystallization, T_c, were determined using the software supplied with the apparatus. Infrared spectra of the powdered glass samples were recorded at room temperature in the range 400–4000 cm^{-1} using a spectrometer (Perkin-Elmer FT-IS, model 1605). These measurements were made on glass powder dispersed in KBr pellets. The dielectric properties have been studied using alternating current measurements, analyzing their dependence on temperature and frequency. The dielectric constant, ε', a.c. conductivity (σ_{ac}) and dielectric loss tangent (tan δ) of the samples were measured in the temperature range 300–650 K, and frequency range (0.12–100 kHz) using a RLC bridge system (Stanford model SR 720 m).

Results and discussion

Density, molar volume, and DTA

Figure 1 shows the relation between the density and molar volume for glass samples as a function of CuO content. From Fig. 1 and Table 1 it can be seen that the density increases monotonically while the molar volume decreases with the increase of CuO content. The variation of density with CuO concentration can be explained by considering the structural changes occurring in the coordination of boron glass network. The structure of crystalline as well as amorphous B_2O_3 is made up of planar $[BO_{3/2}]^0$ triangles [19]. In amorphous B_2O_3, most of these triangles are arranged into boroxyl rings in which three oxygens are part of the ring and three oxygens are outside the ring. These rings are randomly interconnected through loose $[BO_{3/2}]^0$ units. Due to the addition of modifying copper oxide, the

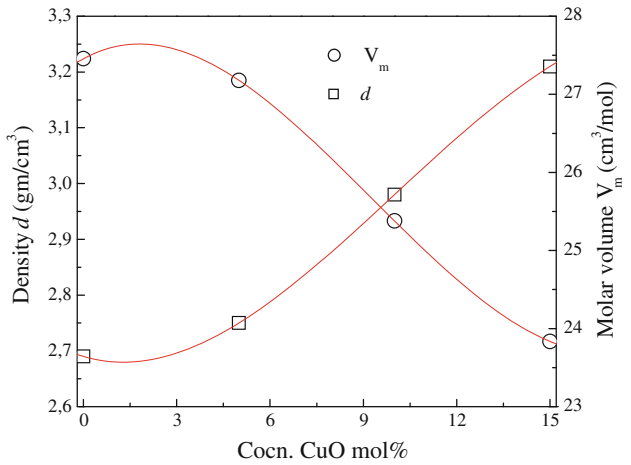

Fig. 1 Variation of density and molar volume with CuO mol%

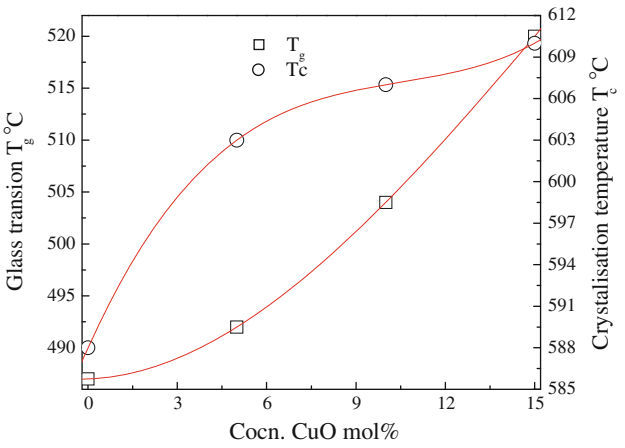

Fig. 2 Variation of glass transition and crystallization temperature as a function of CuO content

three coordinated boron $[BO_{3/2}]^0$ units are converted to four coordinated boron tetrahedral $[BO_{4/2}]^-$ and thus the network dimensionality and connectivity increases [20]. This would lead to efficient packing and compactness in the structure. Also, the increase of density with increase of CuO concentration can be attributed to the replacement of lighter cation B by heavier one Cu cation. From the measured values of T_g, T_c, and the glass-forming ability parameter $(T_c - T_g)$ that gives the information on the stability of the glass against devitrification is evaluate and presented in Table 2. The glass transition temperature (T_g) and crystallization temperature (T_c) as a function of CuO concentration is shown in Fig. 2. It is a fact that T_g is a measure of structural degradation. In the present study, both T_g and T_c increase while $(T_c - T_g)$ decreases with increase in CuO content, indicating the conversion of three coordinated borons into four coordinated borons. These results apparently indicate that with the growing presence of CuO in the glass network copper ions mostly increase the cross-link density and enhance the mean bond strength. The decreasing nature of the glass-forming ability parameter $(T_c - T_g)$ with increasing of CuO indicates an increasing concentration of copper ions that take part in the network modifying positions, and the conversion of BO_4 tetrahedral to BO_3 triangular in the structure.

Table 1 Chemical composition, the density (d), the molar volume (V_m), concentration of copper ions N_i, the inter-mediate distance between copper ions R, polaron radius r_p, respectively, for studied glasses

x (mol%)	Density (g/cm^3)	V_m (cm^3/mol)	Ni (10^{22}/cm^3)	R (Å)	r_p (Å)
0	2.69	27.46	–	–	–
5	2.75	27.18	2.08	1.68	6.79
10	2.98	25.38	2.25	1.64	6.61
15	3.21	23.84	2.43	1.60	6.46

Table 2 Summary of data on DTA differential thermal analysis plots for studied glasses

x (mol%)	T_g (°C)	T_c (°C)	$(T_c - T_g)$ (°C)
0	487	588	101
5	492	603	111
10	504	607	103
15	520	610	90

FT-IR data

The FT-IR spectra of $(15Li_2O–30ZnO–10BaO–(45 - x)B_2O_3–xCuO$ where $x = 0$, 5, 10, and 15 mol%) glasses are presented in Fig. 3. In the infrared spectral region, the

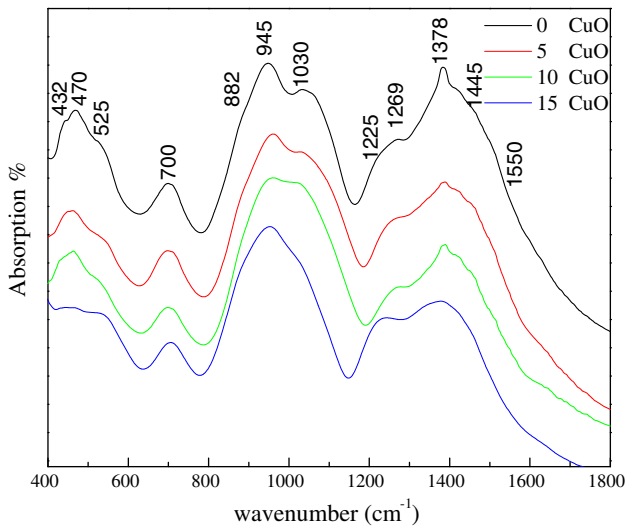

Fig. 3 FT-IR absorption spectra for the studied glasses

vibrational modes of the borate network have three regions [21–23]: (1) bands in the region 1200–1600 cm^{-1} (band due to BO_3 units, i.e., the asymmetric stretching relaxation of the B–O bond of trigonal BO_3 units); (2) bands in the region 800–1200 cm^{-1} (band due to BO_4 units, i.e., the B–O bond stretching of the tetrahedral BO_4 units); 3 Bands in the region 625–725 cm^{-1} (due to the bending of B–O linkages). Thus, the band at 1550 cm^{-1} is due to symmetric stretching relaxation of the B–O band of trigonal BO_3 unit [24], the band at 1445 cm^{-1} is due to B–O^- vibrations [25]. The band at 1378 cm^{-1} due to the B–O–B bridges of trigonal BO_3 units almost remain unchanged in the composition range studied. The two bands around 1225 and 1269 cm^{-1} were assigned to the formation of pyroborate groups. The three bands observed around 1030, 945, and 882 cm^{-1} are due to the B–O bond stretching of tetrahedral BO_4 units [26]. The existence of IR bands in the range 400–600 cm^{-1} indicates the presence of Zn–O tetrahedral bending vibrations in the present glass system [22]. In general, the IR absorption band at 806 cm^{-1} is assigned to the boroxol ring in the borate glass network. In the present study, the peak at 806 cm^{-1} is found missing, which indicates the absence of boroxol ring in the glass network. It is well known that the borate network consists of sp^2 planar BO_3 units and more stable sp^3 tetrahedral BO_4 units. Each BO_4 unit is linked with two such other units and one oxygen from each unit with a metal ion and the structure leads to the formation of long chain tetrahedrons. The presence of such BO_4 units is evident from the IR spectral studies. In general, ZnO is a glass modifier and enters the glass network by breaking up the B–O–B bonds (normally the oxygen of ZnO breaks the local symmetry while Zn^{2+} ions occupy interstitial positions) and introduces coordinate defects known as dangling bonds along with non-bridging oxygen ions. In this case, Zn^{2+} is octahedrally coordinated. However, ZnO may also participate in the glass network with ZnO_4 structural units when zinc ion is linked to four oxygens in a covalency bond configuration [27, 28]. With the introduction of CuO up to 15 mol%, the intensity of the band due to BO_4 units is observed to decrease with a shift of the metacenter towards higher wavenumber while that of BO_3 units is observed to increase with a shift of band position towards lower wavenumber. For further increase in the concentration of CuO, a reversal trend in the intensity of these bands has been observed. The intensity of the band due to ZnO_4 units is observed to be the highest in the spectrum of the glass free CuO and the lowest in the spectrum of the glass containing 15 mol%.

Dielectric properties

The temperature dependence of ε' for the glasses free and containing different concentrations of CuO at 10 kHz is shown in Fig. 4 and at different frequencies for the glass containing 15 mol% of CuO is shown in Fig. 5. The value of ε' is found to exhibit a considerable increase at higher temperatures especially at lower frequencies; the rate of increase of ε' with temperature is found to be the highest for the glass containing 5 mol% of CuO. A comparison plot of variation of tan δ with temperature, measured at a frequency of 10 kHz is presented in Fig. 6. The temperature dependence of tan δ for the glass containing 15 mol% of CuO at different frequencies is shown in Fig. 7. The inset of Fig. 4 gives the variation of ε' at room temperature with the concentration of CuO at 10 kHz. The curves of CuO containing glasses have exhibited distinct maxima; with increasing frequency the temperature maximum shifts

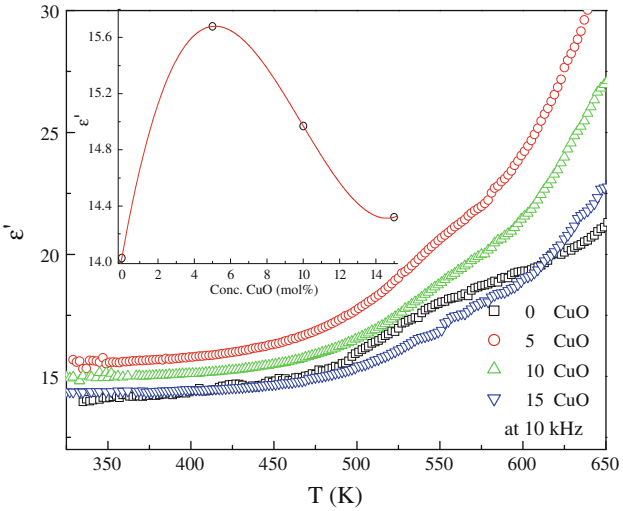

Fig. 4 A comparison plot of variation of dielectric constant with temperature at 10 kHz for studied glasses. *Inset* gives variation of dielectric constant with CuO content at 10 kHz

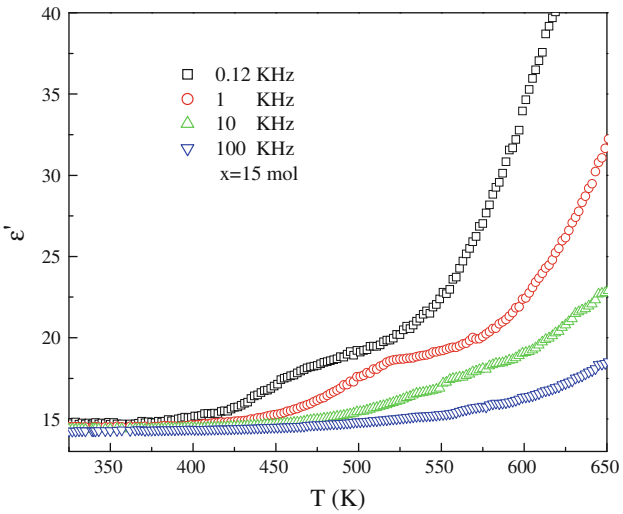

Fig. 5 The variation of dielectric constant with temperature at different frequencies for the sample containing 15 mol% of CuO

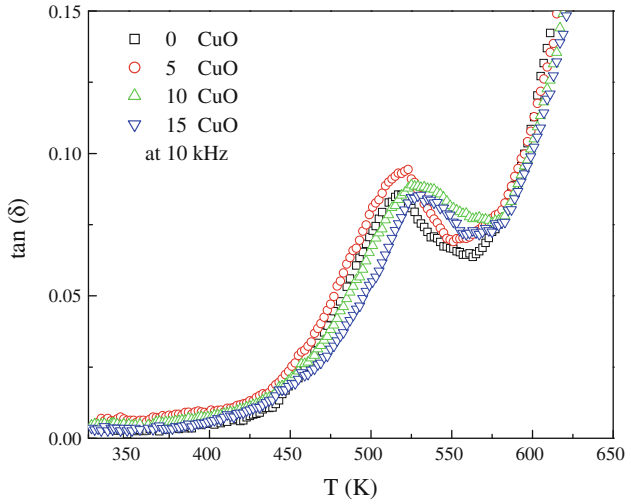

Fig. 6 A comparison plot of variation of dielectric loss with temperature at 10 kHz for studied glasses

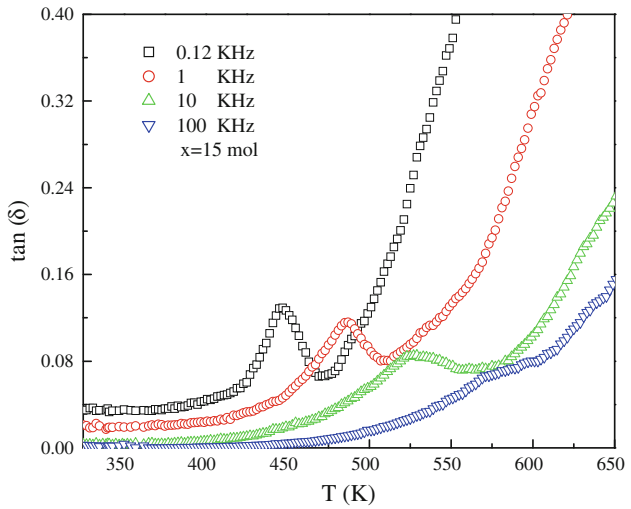

Fig. 7 The variation of tan δ with temperature at different frequencies for the sample containing 15 mol% of CuO

towards higher temperature and with increasing temperature the frequency maximum shifts towards higher frequency, indicating the dielectric relaxation character of dielectric losses of these glasses. Further, the observations on dielectric loss variation with temperature for different concentrations of CuO indicate an increase in the broadness and $(\tan \delta)_{max}$ of relaxation curves with the shifting of the maximum towards higher temperature with increase in the concentration of CuO up to 15 mol%. The effective activation energy W_d for the dipoles is evaluated for all the glass samples using the relation:

$$f = f_0 \exp -W_d/KT \quad (1)$$

where f is the frequency and f_0 a constant, the effective activation energy, W_d, for the dipoles is calculated for all

Table 3 Data on dielectric properties for studied glasses

x (mol%)	W_{ac} (eV)	W_d (eV)	Log σ_{ac} $(\Omega\ m)^{-1}$ at 10 kHz, 300 K	β (radian)
0	0.74	1.44	−17.02	0.588
5	0.47	1.38	−16.63	0.632
10	0.57	1.54	−17.18	0.521
15	0.63	1.67	−18.06	0.455

the glasses and presented in Table 3. The activation energy for dipoles is found to increase with increase in the concentration of CuO. The a.c. conductivity, σ_{ac} is calculated at different temperatures using the equation:

$$\sigma_{ac}(\omega) = \varepsilon_o \omega \varepsilon' \tan \delta \quad (2)$$

where $\tan \delta = \varepsilon''/\varepsilon'$, defines the loss tangent, which is independent of the sample geometry, ε_o is the vacuum dielectric constant. The a.c. conductivity, σ_{ac}, is calculated at different temperatures for these glasses using Eq. 2, for different frequencies and the plot of log σ_{ac} against $1/T$ is shown in Fig. 8 for all glasses at 10 kHz. From these plots, the activation energy for conduction, W_{ac}, in the high temperature region over which a near linear dependence of log σ_{ac} with $1/T$ calculated and presented in Table 3, and inset of Fig. 8; the activation energy is found to decrease with introducing of CuO content up to 5 mol%, and then increase up to 15 mol%, while the a.c. conductivity increases with increase in CuO content up to 5 mol% and then decrease up to 15 mol%. The contribution of electrical polarizations (electronic, ionic, dipolar, and space charge polarizations) to the dielectric constant, the space charge polarization depends on the perfection of the glasses. Recollecting the data on the dielectric properties of

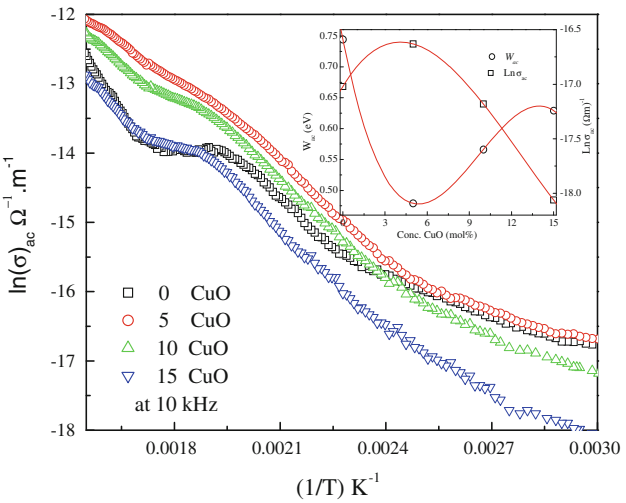

Fig. 8 Variation of log σ_{ac} with $1/T$ at 10 kHz for studied glasses. *Inset* represents the variation of a.c. conductivity at (300 K, 10 kHz) and activation energy with composition

($15Li_2O$–30ZnO–10BaO–$(45 - x)B_2O_3$–xCuO where x = 0, 5, 10, and 15 mol%) glasses, a substantial hike in the values of the dielectric parameters (with respect to those of CuO free glasses) is observed with the increase in the concentrations of CuO up to 5 mol%; such an increase is obviously due to the presence of larger concentration of Cu^{2+} ions; the copper ions act as modifiers similar to Li ions and generate bonding defects by breaking the bonds B–O–B, B–O–Zn, etc. The defects thus produced create easy pathways for the migration of charges that would build up space charge polarization and assist to an increase in the dielectric parameters as observed [29–31].

The dielectric constant and loss vary with the frequency and temperature suggests that these glasses exhibit dielectric relaxation effects. Conventionally, the dielectric relaxation effects are described with the variable frequency at a fixed temperature. However, similar information can also be obtained by analyzing these results at a fixed frequency and at variable temperature as suggested by Bottcher and Bordewijk [32]. Substituting Eq. 1 in standard Debye relations for dielectric relaxation, one can obtain

$$\varepsilon'(\omega, T) = \varepsilon_\infty + 1/2(\varepsilon_s - \varepsilon_\infty)[1 - tgh(E_a/RT + \mathrm{Ln}\omega A)] \quad (3)$$

$$\varepsilon''(\omega, T) = [1/2(\varepsilon_s - \varepsilon_\infty)]/\cosh(E_a/RT + \mathrm{Ln}\omega A) \quad (4)$$

In Eqs. 3 and 4, ε_∞ is temperature independent whereas ε_s is dependent on temperature. Having in mind that the variation of hyperbolic trigonometric functions in Eqs. 3 and 4 with temperature is very minute, these equations can be rewritten as

$$\varepsilon'(\omega, T) = \varepsilon_\infty + 1/2(\varepsilon_s - \varepsilon_\infty)\{1 - tgh[E_a(1/T + 1/T_m(\omega)]/R)]\} \text{ and} \quad (5)$$

$$\varepsilon''(\omega, T) = [1/2(\varepsilon_s - \varepsilon_\infty)]/\cosh[E_a(1/T + 1/T_m(\omega)]/R)] \quad (6)$$

In these equations, $T_m(\omega)$ is the peak temperature where ε' exhibits the maximum value. Thus, as per Eqs. 9 and 10, the plots of $\varepsilon'(\omega, T)$ and $\varepsilon''(\omega, T)$ against $1/T$ should be centro symmetric and symmetric curves, respectively, in the dielectric relaxation region. As an example, for one of the glasses (the sample containing 15 mol% of CuO) under investigation, the variations of $\varepsilon'(\omega, T)$ and $\varepsilon''(\omega, T)$ with $1/T$ is shown in Fig. 9. The shape of these curves is well in agreement with Eqs. 5 and 6 and clearly confirms the relaxation character of dielectric properties of these glasses. Further, to know whether there is single relaxation time or spreading of relaxation times for the dipoles, we have adopted a pseudo Cole–Cole plot method (instead of conventional Cole–Cole plot between $\varepsilon'(\omega)$ and $\varepsilon''(\omega)$ at a fixed temperature) suggested by Sixou et al. [33] in which

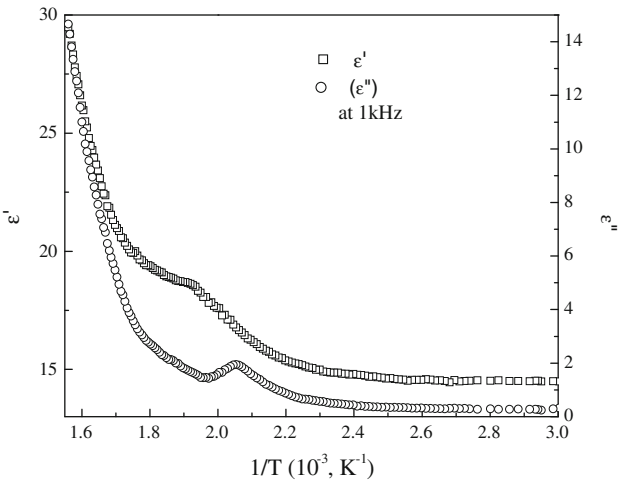

Fig. 9 Variation of $\varepsilon'(\omega, T)$ and $\varepsilon''(\omega, T)$ with $1/T$ for the sample containing 15 mol% of CuO

$\varepsilon'(T)$ versus $\varepsilon''(T)$ can be plotted at a fixed frequency. The nature of variation of $\varepsilon'(T)$ and tan δ with temperature for these glasses indicates that the Cole–Davidson equation:

$$\varepsilon^*(\omega) = \varepsilon_\infty + \left[(\varepsilon_s - \varepsilon_\infty)/(1 - i\omega\tau)^\beta\right] \quad (7)$$

can safely be applied to these glasses. Separating real and imaginary terms of Eq. 7 and rewriting with explicit temperature dependence of terms:

$$\varepsilon'(\omega, T) = \varepsilon_\infty + (\varepsilon_s - \varepsilon_\infty)\left[\cos\varphi(T)^\beta \cos\beta\varphi(T)\right] \quad (8)$$

and

$$\varepsilon'(\omega, T) = (\varepsilon_s - \varepsilon_\infty)\cos\varphi(T)^\beta \sin\beta\varphi(T) \quad (9)$$

where

$$\varphi(T) = \tan^{-1}(\omega\tau) = \tan^{-1}\left(\omega A_o e^{-W_d/KT}\right) \quad (10)$$

In Eq. 10 A_o is a constant and W_d is the activation energy for the dipoles. The plot between $\varepsilon'(T)$ and $\varepsilon''(T)$ specified by Eqs. 8 and 9 at a fixed frequency is often called a pseudo Cole–Cole plot, which cuts ε'-axis at ε_s and ε_∞. Here, ε_s is known as high-temperature dielectric constant and ε_∞ is the low temperature dielectric constant. The plot cuts ε'-axis (as per Sixou) at low temperature side at an angle of $(\pi/2)\beta$, here β is the spreading factor for relaxation times. For the sample containing 15% of CuO, a pseudo Cole–Cole plot at 1 kHz is shown in Fig. 10. The spreading factor β estimated from this plot is 0.456 radians; such plots have also been drawn for all glasses and the value of β is estimated in a similar way; the value of β is found to decrease when the concentration of CuO is introduced in the glass matrix up to 5 mol%, Table 3. Thus the analysis indicates that there are different types of dipoles that are contributing to the relaxation effects in these glasses.

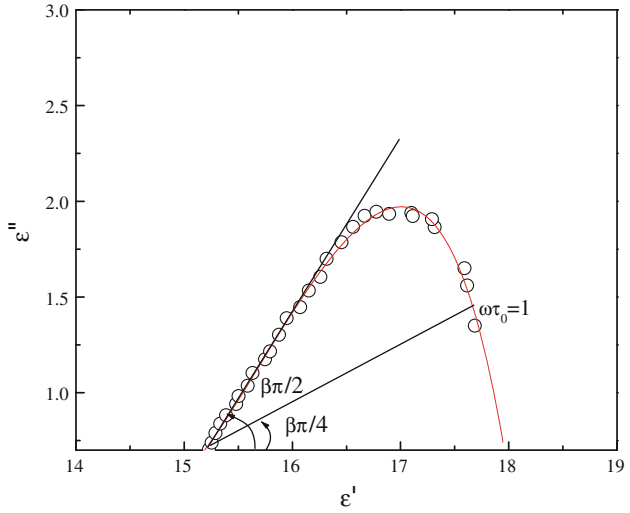

Fig. 10 A pseudo Cole–Cole plot drawn at 1 kHz for the sample containing 15 mol% of CuO

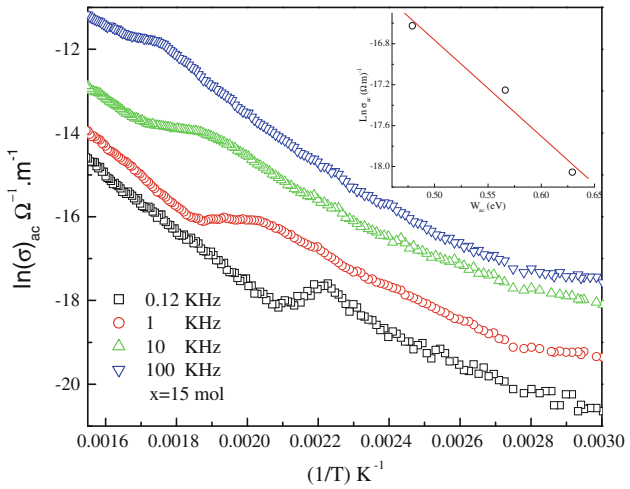

Fig. 11 Variation of log σ_{ac} with $1/T$ at 10 kHz for the sample containing 15 mol% of CuO. Inset represents the variation of conductivity with the activation energy

The spreading of relaxation in CuO containing glasses may be attributed to the conventional divalent copper ions [11, 12]. The shifting of relaxation region towards lower temperatures and decrease in the activation energy for the dipoles with increase in the concentration of CuO from 0 to 5 mol% suggests an increasing degree of freedom for dipoles to orient in the field direction in the glass network. The decrease in the intensity of the relaxation effects beyond 5% of CuO supports the earlier argument that a part of Cu^{2+} ions are converted into Cu^{+} state that takes network forming positions. When a plot is made between log σ_{ac} versus activation energy for conduction (in the high-temperature region) a near linear relationship is observed (inset of Fig. 11); this observation suggests that the conductivity enhancement is directly related to the thermally stimulated mobility of the charge carriers in the high temperature region. The conductivity isotherm as a function of the concentration of CuO passes through a maximum at $x = 5$ mol% (Fig. 8). The figure obviously suggests a type of transition from predominantly ionic to electronic conductivity [34]. With the entry of highly mobile Li ions into the glass network, the electronic paths are progressively blocked causing an inhibition of the electronic current with a simultaneous increase in the ionic transport. A mobile electron, or polarons, involved in the process of transfer from Cu^{+} to Cu^{2+}, is attracted by the oppositely charged lithium ions. This cation polaron pair moves together as a neutral entity. As expected, the migration of this pair is not associated with any net displacement of the charge and thus does not contribute to electrical conductivity; as a result, there is a decrease in the conductivity results beyond 5 mol% of CuO. The low temperature part of the conductivity (a near temperature independent part as in the case of present glasses) up to nearly 390 K can be explained on the basis of quantum mechanical tunneling model [35]. When the concentration of CuO >5 mol% in the glass matrix, the values of ε', tan δ and σ_{ac} are found to decrease (at any frequency and temperature) and the value of activation energy for a.c. conduction is observed to increase; such variation of these parameters may be ascribed to the presence of larger concentration of copper ions in Cu^{+} state that take network forming positions. The presence of such cuprous ions may decrease the degree of disorder in the glass network and as a result we may expect the larger concentration of zinc ions that take network forming positions with tetrahedral ZnO_4 units. Such structural units may alter with BO_4 structural units, increase the rigidity of the glass network and cause to decrease the values of dielectric parameters.

The dielectric parameters of ($15Li_2O$–$30ZnO$–$10BaO$–$(45 - x)B_2O_3$–$xCuO$ where $x = 0$, 5, 10, and 15 mol%) glasses, indicate that the rate of increase of ε' and tan δ with temperature is the highest for the sample containing 5 mol% of CuO and the lowest for the glass sample containing 15 mol% of CuO. These revelations are also consistent with the view that, in the concentration range of 5–15 mol%, the copper and also the zinc ions mostly occupy network forming positions and decrease the degree of disorder in the glass network.

Conclusions

The summary of the results on studies of various physical properties of ($15Li_2O$–$30ZnO$–$10BaO$–$(45 - x)B_2O_3$–$xCuO$ where $x = 0$, 5, 10, and 15 mol%) glasses, is as follows: The analysis of DTA results suggests that the

glass-forming ability is higher for the glasses containing CuO beyond 5 mol%. The analysis of IR results suggests that the glass consists of BO_3, BO_4, and ZnO_4 bridge bands, forming a large glass network. With increasing CuO content, the transition of [BO_4] tetrahedral to [BO_3] triangular happens, which results in the decrease of BO_4 and increase of BO_3 bridge in the structure. The structural changes observed by varying the CuO content in these glasses and evidenced by FTIR investigation suggest that the CuO play a network modifier role in these glasses while ZnO play the role of network formers. The dielectric parameters (viz., ε', $\tan\delta$ and σ_{ac}) are found to increase and the activation energy for a.c. conduction is found to decrease with the increase in the concentration of CuO up to 0.6 mol%. The analysis of dielectric relaxation effects exhibited by these glasses indicated that there is a spreading of relaxation times. The conduction in the high-temperature region seems to be connected with both electronic and ionic. More specifically, up to 5 mol% of CuO, the ionic conduction seems to be dominant while in the higher concentration range, the electronic and ionic conduction seems to prevail.

References

1. Abdel-Baki M, Salem AM, Abdel-Wahab FA, El-Diasty F (2008) J Non-Cryst Solids 354:4527
2. Suzuki T, Hirano M, Hosono H (2002) J Appl Phys 91:41
3. Salem SM (2010) J Alloys Compd 503:242
4. Sreekanth Chakradhar RP, Murali A, Rao JL (2000) Physica B 293:108
5. Kondakova OA, Zylibin AS, Dembovsky SA (2000) Glass Phys Chem 26:418
6. Harami T, Hiramatsu O, Handa K (2000) Phys Chem Glasses 41:333
7. Roling B (1999) J Non-Cryst Solids 244:34
8. Tsuchiya T, Yamakawa H (1990) J Ceram Soc Jpn 98:1083
9. Deshmukh PT, Burghate DK, Deogaonkar VS, Yawate SP, Pakade SV (2003) Bull Mater Sci 26:639
10. Duran A, Fernandez Navarro JM (1985) Phys Chem Glasses 26:126
11. Kumar VR, Veeraiah N (1997) J Phys III 7:951
12. Prasad SVGVA, Sahaya Baskaran G, Veeraiah N (2005) Phys Status Solidi A 202:2812
13. Moustafa YM, Hassan AK, El-Damrawi G, Yevtushenko NG (1996) J Non-Cryst Solids 194:34
14. Nageswara Rao P, Raghavaiah BV, Krishna Rao D, Veeraiah N (2005) Mater Chem Phys 91:381
15. Bellini JV, Morelli MR, Kiminami RHGA (2008) Mater Lett 62:335
16. Thulasiramudu A, Buddhudu S (2006) J Quant Spectrosc Radiat Transfer 97:181
17. Sugita H, Honma T, Benino Y, Komatsu T (2007) Solid State Commun 143:280
18. Saritha D, Markandeya Y, Salagram M, Vithal M, Singh AK, Bhikshamaiah G (2008) J Non-Cryst Solids 354:5573
19. Srinivasa Rao a L, Srinivasa Reddy M, Krishna Rao D, Veeraiah N (2009) Solid State Sci 11:578
20. Abe T (1952) J Am Ceram Soc 35:756
21. Naga Raju G, Veeraiah N, Nagarjuna G, Satyanarayana PVV (2006) J Phys B 373:297
22. Bale S, Rahmana S, Awasthi AM, Sathe V (2008) J Alloys Compd 460:699
23. Zhou L, Lin H, Chen W, Luo L (2008) J Phys Chem Solids 69:2499
24. Lakshminarayana G, Buddhudu S (2006) J Spectrochim Acta A 63:295
25. Alemi AA, Sedghi H, Mirmohseni AR, golsanamlu V (2006) J Bull Mater Sci 29:55
26. Gaafar MS, Abd El-Aal NS, Gerges OW, El-Amir G (2009) J Alloys Compd 475:535
27. Subbalakshmi P, Veeraiah N (2001) Indian J Eng Mater Sci 8:275
28. Shaaban M, Salem SM, Shaltout I (2010) J Mater Sci 45:1837. doi:10.1007/s10853-009-4167-3
29. Srinivasa Reddy M, Sridhar Raja VLN, Veeraiah N (2007) Eur Phys J Appl Phys 37:203
30. Kim SG, Shin H, Park JS, Hung KS, Kim H (2005) J Electroceram 15:129
31. Salem ShaabanM (2009) J Mater Sci 44:5760. doi:10.1007/s10853-009-3807-y
32. Bottcher CJF, Bordewijk P (1978) Theory of electric polarization. Elsevier Scientific Publishing Company, Oxford
33. Sixou P, Dansas P, Gillot D (1967) J Chem Phys 64:834
34. Montani RA, Frechero MA (2003) Solid State Ion 158:327
35. Austin IG, Mott NF (1969) Adv Phys 18:657